Preparation and Characterization of Alginate- Hydroxyapatite Paste for Bone Regeneration

Sudip Dasgupta
Department of Ceramic Engineering
National Institute of Technology, Rourkela, India

Corresponding author- dasguptas@nitrkl.ac.in

Abstract: The objective of the present study was to prepare Si doped hydroxyapatite nanopowder incorporated photocurable aligate paste suitable for orthopaedic application. 0.4 wt% silicon substituted hydroxyapatite nanopowder with average particle size between 85-90 nm was synthesized using wet chemical method. X- ray diffraction and FTIR analysis confirmed substitution of PO_4^{3-} with SiO_4^{4-} groups in prepared HAp nanopowder. On addition of Si into hydroxyapatite lattice, crystallite size of the prepared nanopowder was decreased from 14 nm to 11 nm. XRD results further revealed that alginate became predominantly amorphous with successful methacrylation using methacrylic anhydride. Methacrylate-modified alginate, showed new peaks at 1.8–2.0, 5.7–5.9, 6.1–6.3 ppm due to the presence of methacrylate proton as suggested by NMR studies which further confirmed successful methacrylation of alginate. Methacrylated alginate and Si doped HAp nanopowders were mixed in a weight ratio of 4:1 to prepare a phtocroslinkable paste in presence of 0.5% wt/v photoinitiator such as irgacure. The prepared paste showed good injectability and hardenability on exposure of ~365 nm UV radiation for 10 minutes to give a biopolymer matrix with little open porosity.

1. Introduction

Alginate possesses reversible gelling properties in aqueous solutions due to ionic interactions between divalent cations, such as calcium, barium, and magnesium and carboxylic acid moieties on its guluronic acid residues [1]. Such ionically crosslinked alginate gels despite having several favourable properties, limited control over its mechanical properties, swelling ratios, and degradation profiles demands alternative approach to bridge it in three dimensions. Such deterioration in mechanical and chemical properties in alginate hydrogel mainly stems from uncontrollable loss of divalent cations into the surrounding environment. Instead, intermolecular covalent crosslinking of alginate by means of chemical agents can yield in alginate microcapsules or macroscopic hydrogels with a wide range of mechanical properties. However, such crosslinking reagents and reaction conditions sometimes prove unfavorable or toxic to the encapsulated cells or growth factors [2]. Biomedical application of photocrosslinked hydrogels have recently attracted many researchers because of the prospect of delivering aqueous macromer solutions containing cells and/or bioactive factors in a minimally invasive manner [3-10]. Such hydrogel can rapidly be crosslinked in physiological conditions in situ following brief exposure to ultraviolet (UV) or visible light. Appropriate choice of a photoinitiator and short exposure to low-intensity light can lead to photopolymerization to occur with limited deleterious effects to cells and bioactive molecules [11]. Moreover, degree of crosslinking of alginate can be varied with intensity and exposure time of light. This gives scope to tune mechanical properties, swelling ratio as well as degradation of alginate matrix in physiological environment.

As extracellular matrix of bone is considered to be a composite made of inorganic and organic hybrid network, appropriate choice of biopceramic phase in combination with photocurable hydrogel can result in an ideal bone substitute material. Hydrogel (HG)/calcium phosphate (CaP) composites with in situ gelation triggered by chemistry that have been investigated recently [12-15]. Silated HPMC [12, 13] and aldehyde-modified hyaluronic acid as matrices in combination with hydrazide-modified polyvinyl alcohol [14] has been reported. Recently, Lin et al. [16] designed composites consisting of HA and a poly(ethylene glycol) (PEG) copolymer, namely poly(lactic acid-co-glycolic acid)–g-PEG. Possible interactions between biphasic calcium phosphate (BCP) and hydroxy propyl methyl cellulose (HPMC) have been investigated in injectable bone substitute (IBS) composites [17], however, within the sensitivity of the employed measurement techniques, no chemical bonding between BCP and HPMC was detected.[17]. Thus inducing interactions between polymer matrix and CaP particles to promote uniform dispersion of mineral phase throughout the matrix and prevention of CaP particle agglomeration within the matrix are a critical challenges for development of CaP-hydrogel injectable for bone tissue engineering.

Our objective is to develop an injectable as well as photocurbale artificial bone substitute material comprising of hydroxyapatite nanoparticles embedded in photcurbale alginate based matrix. As fundamental structural unit of bone is hydroxyapatite nanoparticles embedded in triple helix collagen fibre, our hypothesis is to mimic the natural composition of bone by intimately mixing surface modified Si doped hydroxyapatite nanoparticles in natural biopolymer like alginate matrix.

2. Materials and Methods

2.1 Materials

All reagents and precursors such as methacrylic anhydride(MA, $[H_2C=C(CH_3)CO]_2O$, (94%, Aldrich, USA), sodium alginate (Merck, India), Calcium Nitrate $[Ca(NO_3)_2, 4\ H_2O]$ (Merck, India), di-ammonium hydrogen Phosphate $[(NH_4)_2HPO_4]$ (Merck, India), Tetra ethyl ortho silicate [TEOS] (Merck, India), 2-Hydroxy-4′-(2-hydroxyethoxy)-2-methylpropiophenone (Irgacure 2959, 98%, Aldrich, USA) were of analytical grade and used as purchased. All preparations and syntheses were performed at room temperature (RT, 25 ± 2) °C unless otherwise specified.

2.2 Synthesis of Si-doped HA nanoparticles

Si doped HAp was prepared by wet chemical method reported by Gibson et al. The starting precursor materials at the Ca/(P+Si) ratio of 1.67 were mixed and 0.4 wt% of Si was introduced using TEOS as Si source with continuous stirring of resulting suspension for 24 hours. The precipitate was filtered and dried at 60ºC over night in an oven. Figure 1 illustrates the preparation process of Si-doped HAp powder.

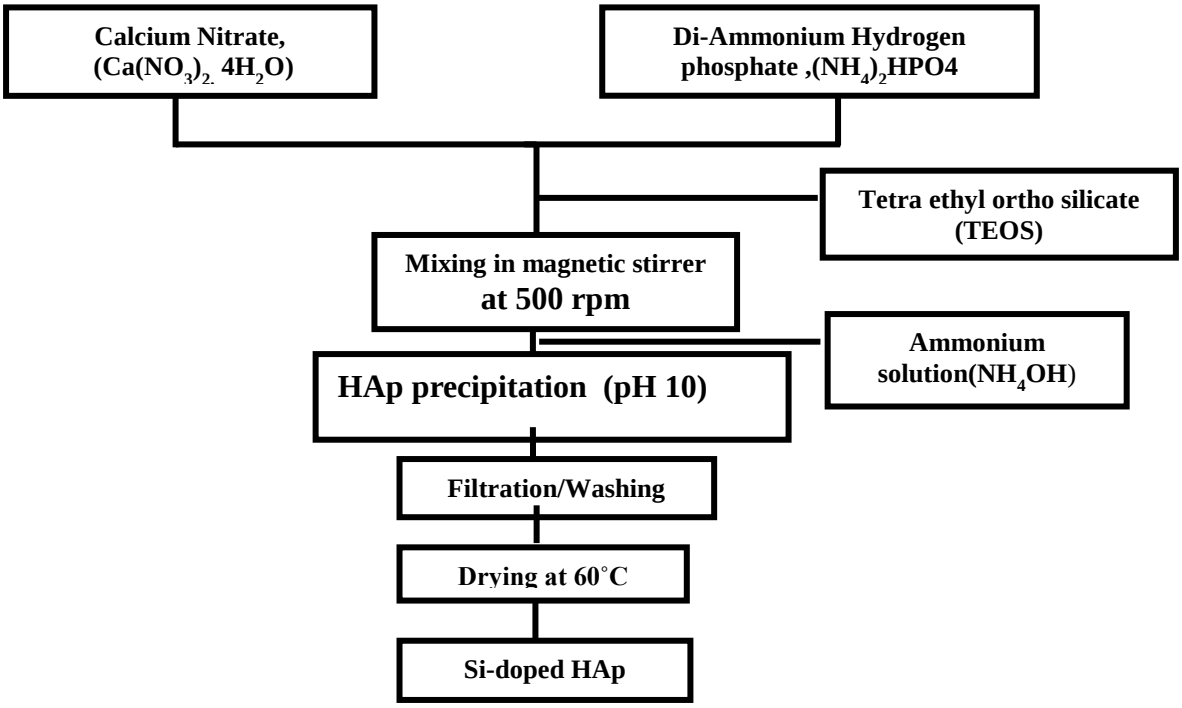

Figure 1: Flow chart of synthesized Si-doped HAp powder using wet chemical method.

2.3 Synthesis of methacrylated alginate

Methacrylated alginate was prepared by reacting low molecular weight alginate with methacrylic anhydride at 4ºC temperature. Methacrylic anhydride (20-fold excess) was added dropwise into a 1% w/v solution of low molecular weight of sodium alginate (37,000 g/mol) in deionized water. The pH of solution was adjusted to 8.0 with 5 M ammonium hydroxide solution. After reacting for 48 h, the macromer solution was dialyzed (molecular weight cut-off=10 kDa) against deionized water for at least 3 days. Methacrylated alginate was purified by dialysis against diH_2O (MWCO 3500; Spectrum Laboratories Inc., Rancho Dominguez, CA, USA) for 3 days, filtered (0.22 mm filter), and lyophilized. Figure 2 describes the preparation process of methacrylated alginate.

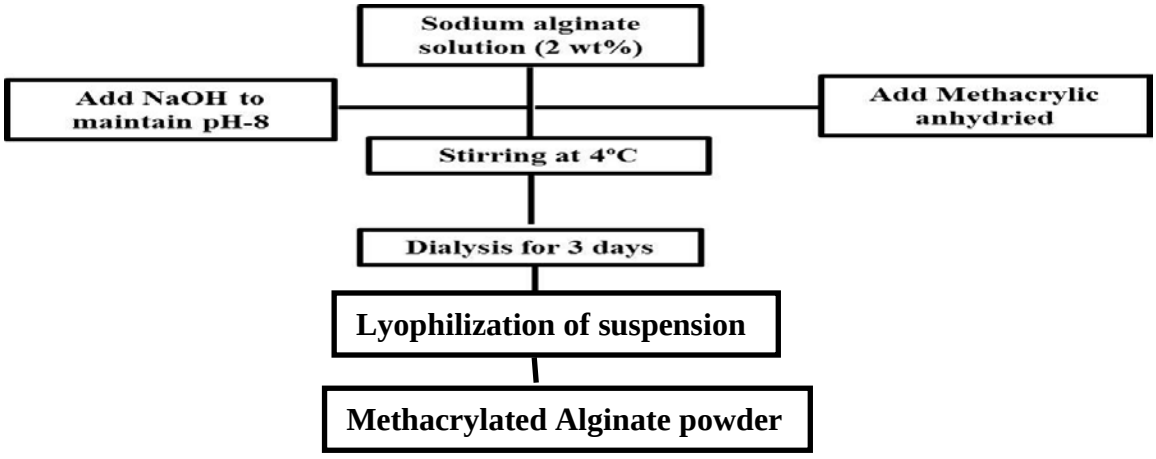

Figure2: Flow diagram of synthesized methacrylated alginate powder.

2.4 Preparation of Alginate-Hydroxyapatite paste and Photocrosslinking

To fabricate photocrosslinked alginate hydrogels, methacrylated alginate (0.2 g) and Si –HAp nanopowders (0.05 gm) were dissolved in 10 ml diH_2O with 0.05% w/v photoinitiator (Irgacure 2959, Sigma). The resultant suspension was injected between two glass plates separated by nearly 1 mm spacers and photocrosslinked using 365 nm UV light at ~10 mW/cm^2 for 8 min to form the hydrogels. Thus obtained photocrosslinked hydrogel paste was dried in incubator at 37.4 ^{o} C for 24 hours and used for further characterization.

3. Characterization

3.1 X-ray diffraction (XRD)

The phases of synthesized doped and undoped hydroxyapatite nanopowders and methacrylated alginate were analysed using X-ray diffraction (XRD) with fully automated X-ray diffractometer (Philips PAN analytical, USA) fitted with Ni-filter. The diffraction patterns were obtained with the help of a XRD analyser using CuKα radiation (λ = 1.542 nm) at 35 kV and 10 mA. Samples were preferably scanned from 20^o to 70^o in 2θ (where θ is the Bragg angle) in a continuous mode with a scanning speed of 0.02 degree/sec.

3.2 Fourier transform infrared spectroscopy (FTIR)

Characteristic functional groups in pure and doped HAp were analysed using Fourier transform infrared (FTIR) (PerkinElmer, USA) spectroscopy. The pellet was prepared by mixing 2 mg of the sample with 200 mg of IR grade KBr at a pressure of 3 ton for FTIR measurement. The absorption spectra were measured using UV spectrometer in the wave number between 4000 to 400 cm^{-1} with a resolution of 1 cm^{-1}.

3.3 Particle size measurement of synthesized nanopowders

Particle size and distribution of synthesized hydroxyapatite powder was estimated using dynamic light scattering technique with the help of zetasizer (Zetasizer nano zs, Malveron). The refractive index for HAp nanopowders and water were considered as 1.65 and 1.33 respectively. Very dilute suspension of 0.01 wt% of synthesized HAp in disilled water was prepared and ultrsonicated for 10 minutes to disperse the particles and then used for particle size analysis.

2.3. ^{1}H NMR characterization

Deuterium oxide was used as a solvent to dissolve methacrylated alginate with addition of 0.05% w/v photoinitiator and placed in a NMR tube. The solution was photocrosslinked at 365 nm UV light at ~ 10 mW/cm^2 for 8 min to form a hydrogel. The ^{1}H NMR spectra of the photocrosslinked alginate hydrogel were recorded on a ultrashield-400 (300 MHz) NMR spectrometer (Bruker, UK). To understand the methacrylation efficiency of alginate, ^{1}H NMR spectra were also used for uncrosslinked, unmodified alginate.

2.4 Scanning electron microscopy (SEM)

Particle size of synthesized Si doped HAp nanopowder and microstructure of the hardened paste were analysed using field emission scanning electron microscopy (FESEM) Novanano

450, FEI, USA). The surface of the sample to be investigated was gold coated using sputter coater (FEI, USA), and then placed inside the FESEM chamber.

4. Results and Discussion

Figure 3 shows XRD pattern of the powders prepared using wet chemical method. The silicon doping did not appear to affect the diffraction pattern of hydroxyapatite. The pattern of the all samples appeared to be identical, without secondary phase, such as TCP or SiO_2 [Figure 3(a), (b)]. All the diffraction peaks of samples corresponded to phase pure hydroxyapatite. However, these reflections became slightly broad and less intense with addition of TEOS [Figure 3(b)]. The result of degradation of crystallinity attributed to the formation of hydroxyl ion vacancy caused due to the substitution of PO_4^{3-} by SiO_4^{4-} with consequent decrease in crystallite size.

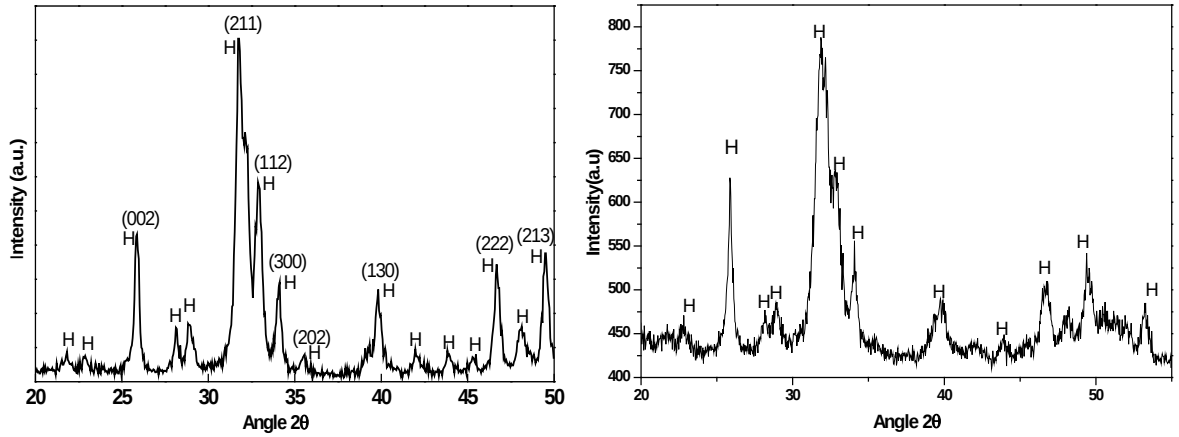

(a) **(b)**

Figure 3(a). XRD patterns of synthesized HAp (b) Si-HAp using wet chemical method.

Table 1: Crystal size and Zeta potential of synthesized hydroxyapatite particle**.**

Parameter	**HAp (A^o) (Theoretical value)**	**Synthesizd HAp (A^o)**	**HAp-Si (A^o)**
a,b	**9.464**	**9.4248**	**9.3996**
c	**6.856**	**6.8862**	**6.8740**
Crystallite Size	**----------**	**140 A^o= 14 nm**	**117 A^o=11.7 nm**
Zeta potential in deionized water of pH-6.8	**----------**	**-6 mV**	**-5.2mV**

Crystallite size calculated from XRD patterns of Si doped and undoped HAp powders using Debye Scherer equation showed a lower value for doped HAp. At the same time, doped HAp nanopowders exhibited a lower zeta potential at pH- 6.8 as compared to undoped HAp

powders that might be because of higher degree of vacancy in hydroxyl ions in the former as compared to the later.

FTIR was evaluated to confirm the effect of silicon substitution on different functional groups, such as hydroxyl and phosphate of hydroxyapatite. Figure 4 shows the FTIR spectra of prepared Si doped HAp sample. First, the bands at 3456 cm^{-1} and 547 cm^{-1} corresponded to the hydroxyl group stretching and vibrational modes, respectively. The bands at 953 cm^{-1} corresponded to P-O stretching vibration modes. The asymmetric stretching vibration of phosphate (v3 PO_4^{3-}) in HAp appeared at 1024 cm^{-1}, whereas the band at 1034 and 1634 cm^{-1} appeared due to the presence of symmetric stretching vibration of phosphate (v_3 PO_4) and carbonate. A new band appeared at 821 cm^{-1} was assigned to Si-O-Si vibration modes of SiO_4^{4-} groups which was polymerized [18] .These result suggest that incorporation of silicon into some of the phosphorous sites in the lattice of HAp resulted in changes in the bonding and symmetry of the phosphate groups, as excess charge was compensated by loss of OH^-.

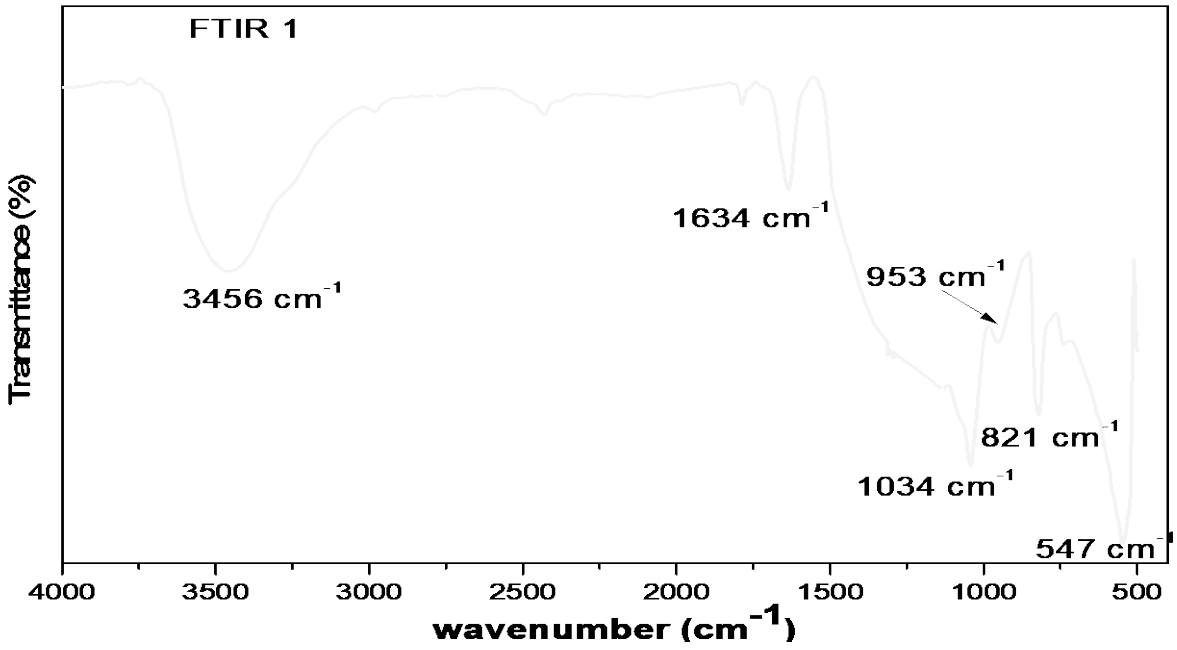

Figure. 4: FTIR spectra of synthesized Si-HAp nanopowder.

Figure.5 represents DLS particle size measurement data of synthesized Si doped HAp nanopowder. An average particle size of 85± 9.5 nm was obtained from DLS measurement which was little bit higher as compared to the particle size shown in the FESEM image in Figure 6(a). Particle size measurement by DLS technique shows hydrodynamic diameter of the particle. Also Si doped HAp particles were to some extent in agglomerated state in the suspension used for DLS measurement that was responsible for higher average particle size value in the DLS measurement.

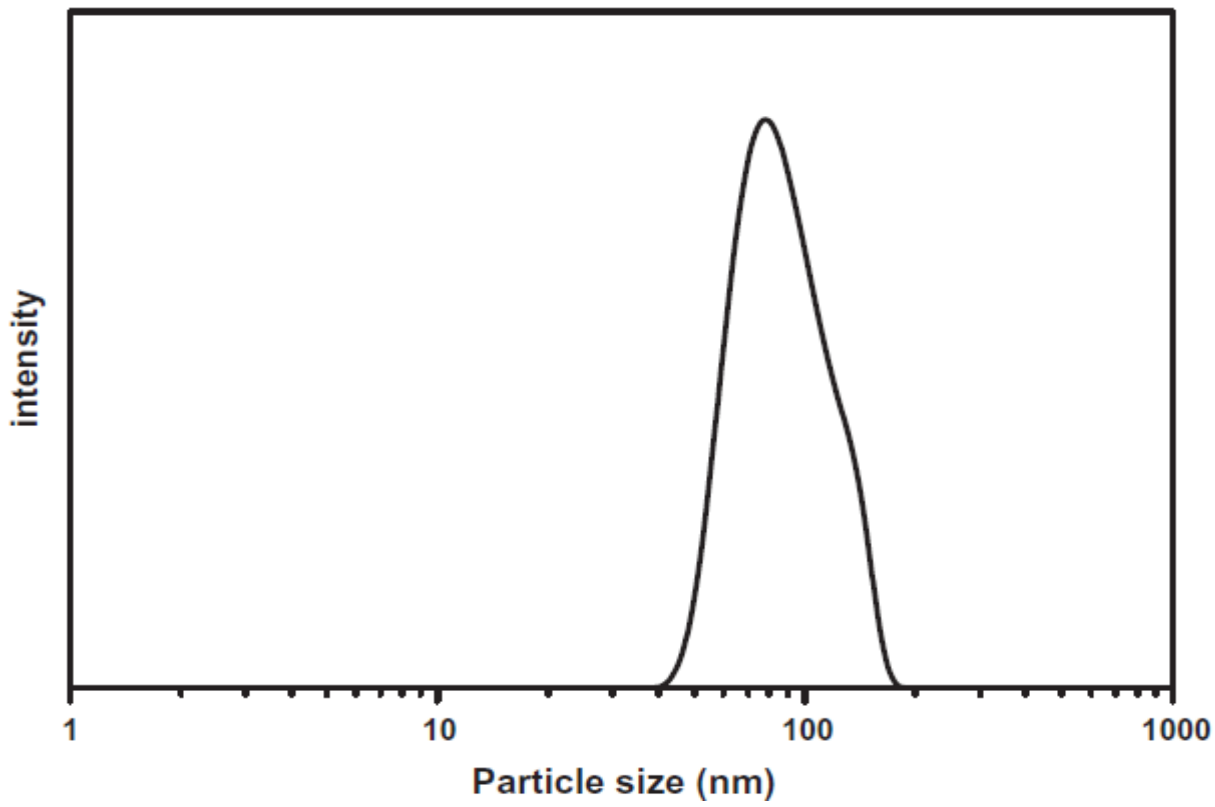

Figure 5. DLS measurement of particle size distribution of Si doped HAp.

From FESEM micrograph in Figure.6 it is evident that the Si-HAp particles were morpologically nearly spherical and agglomerated in course of drying at 60 ^{o}C . EDS analysis in Figure 6 (b) suggests that the synthesized powder with a molar composition of Ca:P=1.65 closely resembled the theoritical composition of HAp.

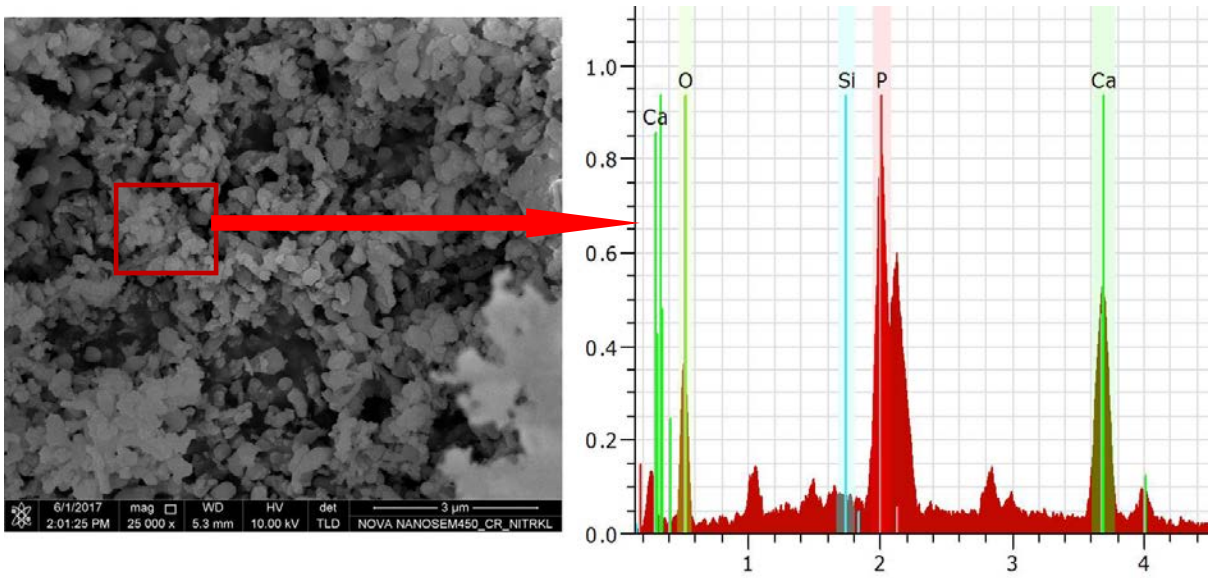

Figure6. Synthesized Si doped n-HAp powder (a) FESEM micrograph (b) EDX analysis

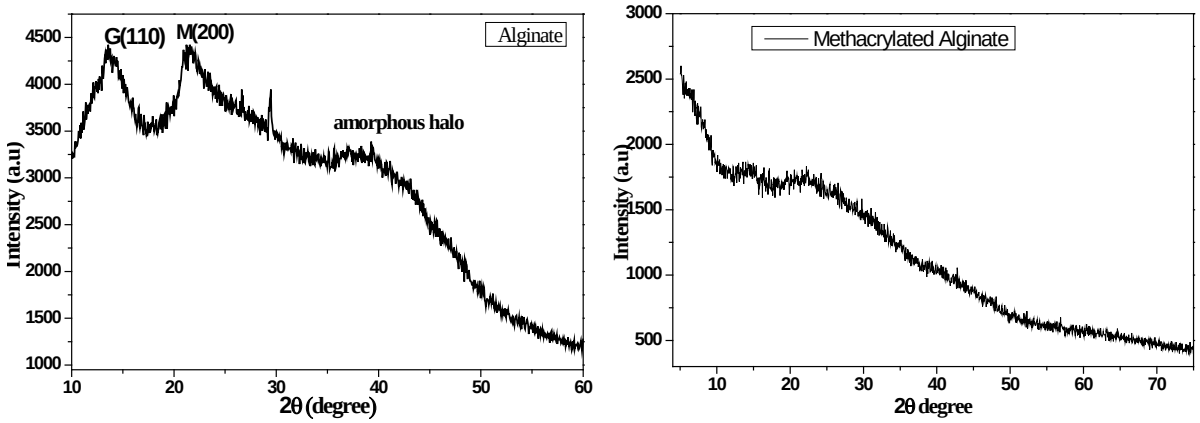

(a) **(b)**

Figure 7. XRD patterns of (a) sodium alginate (b) methacrylated alginate

Figure 7 represents the XRD patterns of sodium alginate and methacrylated sodium alginate. Sodium alginate is usually crystalline due to strong interaction between the alginate chains through intermolecular hydrogen bonding. Three diffraction peaks at 2θ values of 14.1º, 21.5º and 37.4º were observed for sodium alginate [Figure 7(a)] due to the reflection of their (110) plane from polyguluronate unit, (200) plane from polymannuronate, and the other from amorphous halo. [19] In case of methacrylated sodium alginate (Figure 7(b)), the intensity of diffraction peaks of alginate decreased notably which indicates that alginate became predominantly amorphous because of methacrylation. Hydroxyl functional groups in alginate those are responsible for hydrogen bonding formed covalent chemical bond during methacrylation and thus crystalline peaks of diffractogram of sodium alginate was not appeared after methacrylation.

The successful methacrylate modification was confirmed by comparing the ^{1}H NMR spectra of methacrylate-modified alginate in Figure 8. For the methacrylate-modified alginate, new peaks at 1.8–2.0, 5.7–5.9, 6.1–6.3 ppm appeared, that were the methacrylate proton peaks.

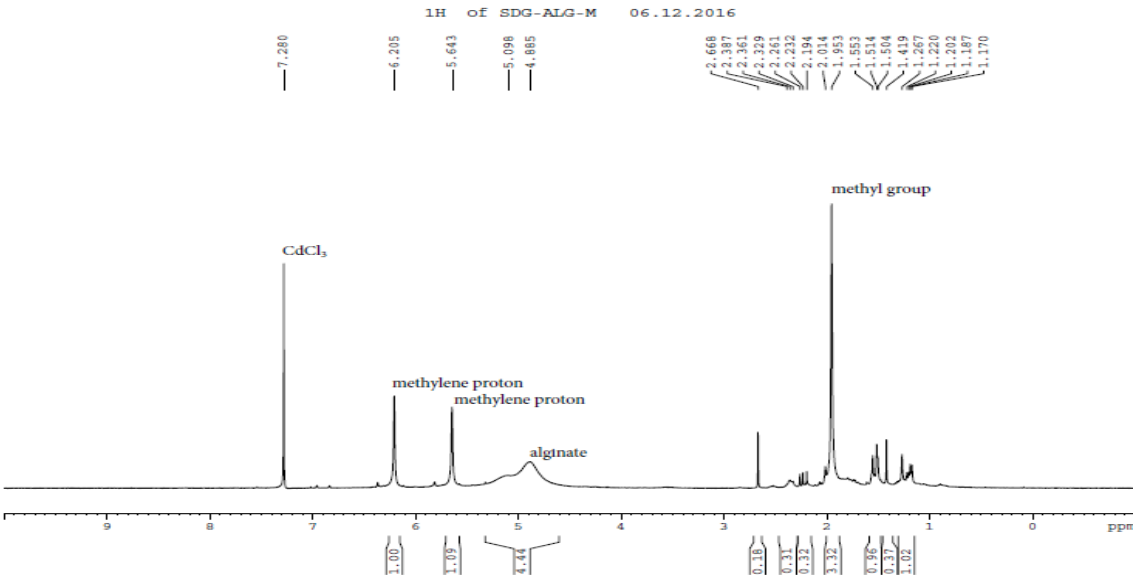

Figure 8. The ^{1}H NMR spectrum of methacrylate-modified alginate polymer . The new peaks δ= 6.19 ppm and 5.73 ppm were the methylene protons and the peak δ= 1.89 ppm was the methyl group peak.

Figure 9 (a) represents the injectable sample prepared from the combination of Si doped HAp and methacrylated alginate in 1:4 weight ratio in 2.5 wt% suspension in D.I. water. Irgacure 2959 was added as a photiniatiator to bridge the monomeric units and harden the paste on exposure to UV radiation for definite time period. The microstructure of the photocrosslinked and hardened paste was shown in Figure 9(b), which shows very little degree of open pores that is good for higher mechanical strength of the paste for early load bearing in the bony defect.

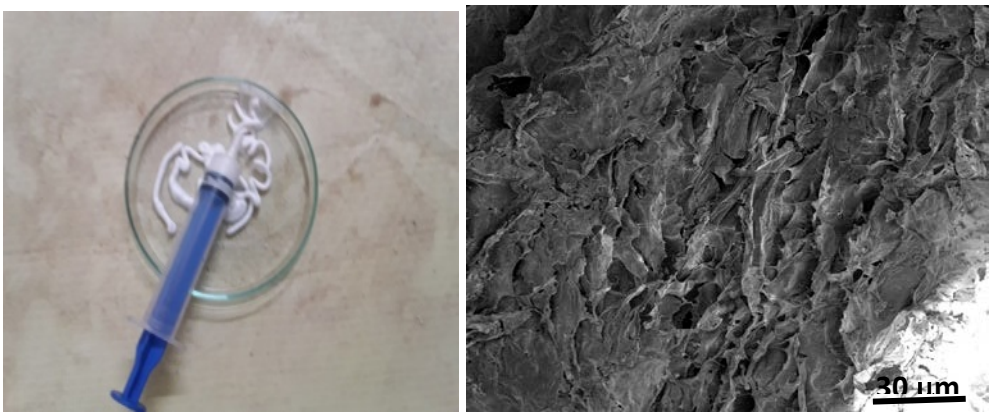

(a) (b)

Figure 9. (a) Injectable Si-doped HAp-methylated alginate paste (b) microstructure of hardened scaffold after UV curing.

Conclusions

In this study, we focused on the synthesis and comprehensive characterization of Si doped HAp and methacrylated alginate used for the preparation of photocrosslinkable biopolymer-ceramic paste for bone tissue engineering. Si doped hydroxyapatite nanopowder was successfully synthesized by substitution of PO_4^{3-} with SiO_4^{4-} groups. Methacrylation of alginate was successfully carried out after reacting alginate with methacrylic anhydride to make alginate matrix photocurable. Si doped HAp nanopowder incorporated alginate based paste showed good injectability and hardened after UV exposure to generate a sparsely porous matrix.

Acknowledgement

The author expresses his warm gratitude for financial support from Council of Scientific and Industrial Research (CSIR) [grant no 22/704/15/EMR-II] for carrying out above research work. Experimental help from Dr. Kanchan Maji for carrying out above research work is sincerely acknowledged.

References

[1] T. Coviello, P. Matricardi, C. Marianecci, F. Alhaique “Polysaccharide hydrogels for modified release formulations”, J Control Release, 119 (1) (2007), pp. 5-24

[2] Birnbaum S, Pendleton R, Larsson PO, Mosbach K. Covalent stabilization of alginate gel for the entrapment of living whole cells. Biotechnol Lett1981;3(8):393–400

[3] C.A. Simmons, E. Alsberg, S. Hsiong, W.J. Kim, D.J. Mooney, “Dual growth factor delivery and controlled scaffold degradation enhance in vivo bone formation by transplanted bone marrow stromal cells”, Bone, 35 (2) (2004), pp. 562-569

[4] H.J. Kong, D.J. Mooney, “The effects of poly(ethyleneimine) (PEI) molecular weight on reinforcement of alginate hydrogels”, Cell Transplant, 12 (7) (2003), pp. 779-785

[5] E. Alsberg, K.W. Anderson, A. Albeiruti, R.T. Franceschi, D.J. Mooney, “Cell-interactive alginate hydrogels for bone tissue engineering” , J Dent Res, 80 (11) (2001), pp. 2025-2029

[6] E. Alsberg, H.J. Kong, Y. Hirano, M.K. Smith, A. Albeiruti, D.J. Mooney, “Regulating bone formation via controlled scaffold degradation”, J Dent Res, 82 (11) (2003), pp. 903-908

[7] A. Atala, W. Kim, K.T. Paige, C.A. Vacanti, A.B. Retik, “Endoscopic treatment of vesicoureteral reflux with a chondrocyte-alginate suspension”, J Urol, 152 (2) (1994), pp. 641-643

[8] S.X. Hsiong, P. Carampin, H.J. Kong, K.Y. Lee, D.J. Mooney “Differentiation stage alters matrix control of stem cells”, J Biomed Mater Res A, 87A (1) (2008), p. 282

[9] A. Yasuda, K. Kojima, K.W. Tinsley, H. Yoshioka, Y. Mori, C.A. Vacanti “In vitro culture of chondrocytes in a novel thermoreversible gelation polymer scaffold containing growth factors”, Tissue Eng, 12 (5) (2006), pp. 1237-1245

[10] N. Cheng, E. Wauthier, L.M. Reid “Mature human hepatocytes from ex vivo differentiation of alginate-encapsulated hepatoblasts”, Tissue Eng Part A, 14 (1) (2008), pp. 1-7

[11] Fisher JP, Dean D, Engel PS, Mikos AG. Photoinitiated polymerization of biomaterials. Ann Rev Mater Res 2001;31:171–81.

[12] Trojani C et al. Ectopic bone formation using an injectable biphasic calcium phosphate/Si-HPMC hydrogel composite loaded with undifferentiated bone marrow stromal cells. Biomaterials 2006;27(17):3256–64.

[13] Sohier J, Corre P, Weiss P, Layrolle P. Hydrogel/calcium phosphate composites require specific properties for three-dimensional culture of human bone mesenchymal cells. Acta Biomater 2010;6(8):2932–9.

[14] Hulsart-Billström G et al. Calcium phosphates compounds in conjunction with hydrogel as carrier for BMP-2: a study on ectopic bone formation in rats. Acta Biomater 2011;7(8):3042–9.

[15] Fatimi A, Tassin JF, Turczyn R, Axelos MA, Weiss P. Gelation studies of a cellulose-based biohydrogel: the influence of pH, temperature and sterilization. Acta Biomater 2009;5(9):3423–32.

[16] Lin G, Cosimbescu L, Karin NJ, Tarasevich BJ. Injectable and thermosensitive PLGA-g-PEG hydrogels containing hydroxyapatite: preparation, characterization and in vitro release behavior. Biomed Mater 2012;7(2): 024107.

[17] Dorozhkin SV. Is there a chemical interaction between calcium phosphates and hydroxypropylmethylcellulose (HPMC) in organic/inorganic composites? J Biomed Mater Res 2001; 54:247-55.

[18] I. Rehman and W. Bonfield, “Characterization of hydroxyapatite and carbonated apatite by photo acoustic FTIR spectroscopy”, J. Mater. Sci. Mater. Med.8 (1) (1997)

[19] Y. Dong, W. Dong, Y. Cao, Z. Han, Z. Ding, “Preparation and catalytic activity of Fe alginate gel beads for oxidative degradation of azo dyes under visible light irradiation”, Catalysis Today, 175 (2011), pp. 346-355